Multicomponent Self-Assembly of a Pentanuclear Ir-Zn Heterometal-Organic Polyhedron for Carbon Dioxide Fixation and Sulfite Sequestration

Xuezhao Li, Jinguo Wu, Cheng He,* Rong Zhang and Chunying Duan

State Key Laboratory of Fine Chemicals, Dalian University of Technology, Dalian, 116023, P. R. China

E-mail: hecheng@dlut.edu.cn

1. Materials and Methods.

2. Syntheses and Characterizations.

3. Single Crystal Analyses of the Complexes.

4. Luminescent Spectra of the Compounds and the Tracing of Transformation

5. References.

1. Materials and Methods

Unless stated otherwise, all chemicals were of reagent grade quality obtained from commercial sources and used without further purification. Acetonitrile (CH_3CN; Aldrich, 99.9+%) were distilled over CaH_2 prior to use. $^{13}CO_2$, 99%, (1% ^{18}O) was purchased from Beijing Gaisi Chemical Gases Center. All reactions were carried out under a nitrogen atmosphere, unless stated otherwise. The elemental analyses of C, H and N were performed on a Vario EL III elemental analyzer. ^{1}H NMR and ^{13}C NMR spectra were measured on a Varian INOVA 400 M and 100 M spectrometer. ESI mass spectra were carried out on a HPLC-Q-Tof MS spectrometer using methanol asmobile phase. Uv-*vis* spectra were measured on a HP 8453 spectrometer. The solution fluorescent spectra were measured on JASCO FP-6500. Abbreviations: ppy = 2-(4-Nitrophenyl)pyridine; nm = nanometres; min = minute(s); h = hour(s); rt = room temperature (20 °C).

2. Syntheses and Characterizations

2.1 Synthesis of *fac*-Ir-NH_2

Ligand *fac*-Ir-NH_2 was synthesized according to the reported procedure with modifications to improve both yields and purities.[S1] All synthetic procedures involving $IrCl_3 \cdot xH_2O$ and other Ir(III) species were performed under an inert N_2 atmosphere and dark environment.

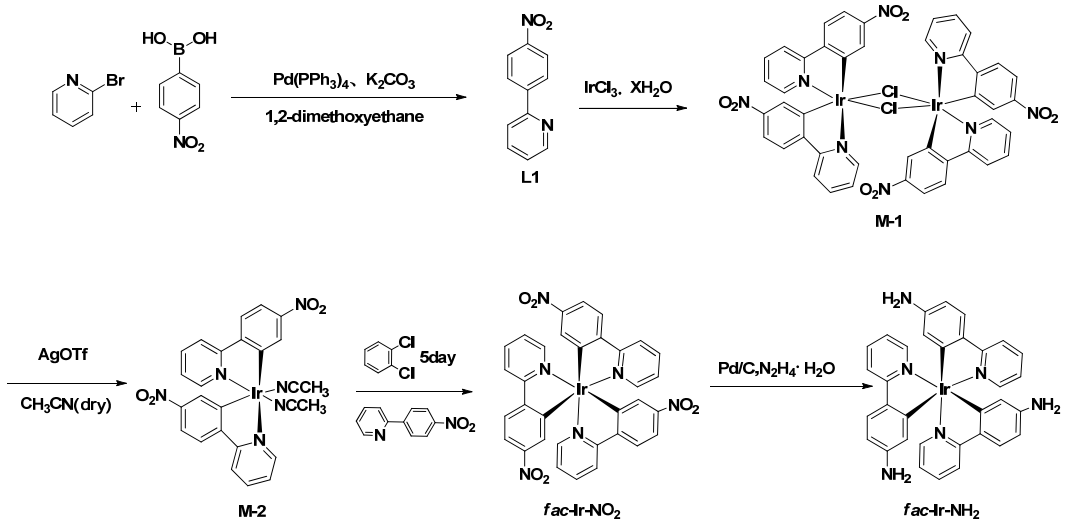

Scheme S1. Synthesis of *fac*-Ir-NH_2.

Synthesis of $[Ir(ppy)_2(\mu\text{-}Cl)]_2$ (M-1)

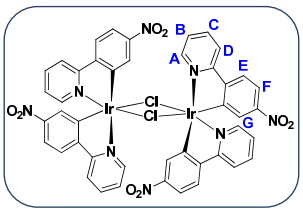

$IrCl_3 \cdot xH_2O$ (0.6 g, 2 mmol) was refluxed with 2.5 equiv of cyclometalating ligand $\mathbf{L_1}$ (1.0 g, 5 mmol) in a 3:1 mixture of 2-methoxyethanol and water, and the reaction mixture was stirred for 24 h at 120 °C. The reaction mixture was filtered, washed with water and ethanol. The red solids were collected and dried under vacuum to give the product **M-1** (0.96 g, yield 77%). ^{1}H NMR (CD_2Cl2-d_2, ppm): δ 9.23 (d, J = 4.6 Hz, 1H, H_A), 8.14 (d, J = 7.1 Hz, 1H, H_G), 8.05 (m,1H, H_E), 7.73 (d, J = 8.6 Hz,1H, H_F), 7.68 (m, 1H, H_B), 7.09 (m, 1H, H_C,), 6.59 (d, J = 2.2 Hz, 1H, H_D).

Synthesis of $[Ir(ppy)_2(NCCH_3)_2]OTf$ (M-2)

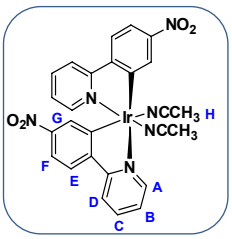

Compound **M-1** (0.25 g, 0.2 mmol) in 75 mL of dry acetonitrile was heated to dissolve all of the chloro-bridged dimer. A 50 mL acetonitrile solution of AgOTf (0.1g, 0.41 mmol) was added to the solution. The mixture was kept at 60°C in the dark for 2 h resulted in a gray precipitate. The gray AgCl precipitate was filtered over a Celite pad resulted a yellow solution. The solution was concentrated in vacuo, then redissolved in a minimal amount of acetonitrile and precipitating with diethyl ether. The yellow crystal precipitate were collected and dried under vacuum to give the product **M-2** (0.3 g, yield 91%). ^{1}H NMR (CD_3CN-d_3, ppm): δ 9.20 (d, J = 8.0 Hz, 1H, H_A), 8.29 (d, J = 8.0 Hz, 1H, H_G), 8.24 (m, 1H, H_E), 7.90 (d, J = 8.0 Hz, 1H, H_F), 7.76 (m, 1H, H_F), 7.69 (m, 1H, H_C), 6.75 (d, J = 4.0 Hz, 1H, H_D), 1.96 (s, 3H, H_H).

Synthesis of *fac*-Ir-NO_2

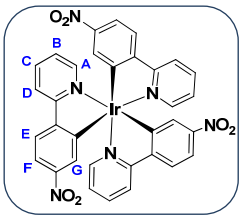

Compound **M-2** (0.25 g, 0.3 mmol) and **L1** (0.066 g, 0.33 mmol) were combined in 15 mL of o-dichlorobenzene and heated at 120 °C under N_2 atmosphere for 100 h. After cooling to room temperature, the reaction solution was chromatographed on a silica gel column packed with petroleum ether to first elute o-dichlorobenzene. Switching to 1 : 1 dichloromethane / petroleum ether eluted the product, as a bright red band in 40% yield. ^{1}H NMR ($CDCl_3$, ppm): δ 8.05 (d, J = 8.0 Hz, 1H, H_A), 7.80 (m, 3H, $H_{B,C,D}$), 7.58 (d, J = 8.0 Hz,1H, H_E), 7.44 (s, 1H, H_G), 7.07 (m, 1H, H_F). ESI-MS [M^+ = 790.2701, $(M+Na)^+$ = 813.2615].

Synthesis of *fac*-Ir-NH_2

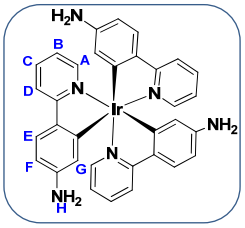

The catalyst Pd/C(10%) and hydrazine hydrate (80%, 15 equiv) were used for reduction ***fac*-Ir-NO_2** to ***fac*-Ir-NH_2**, and dichloromethane was chosen as the solvent (~100% yield). ^{1}H NMR ($CDCl_3$, ppm): δ 7.65 (d, J = 8.0 Hz, 1H, H_A), 7.37-7.45 (m, 3H, $H_{C,D,E}$), 6.67 (m, 1H, H_B), 6.28 (s, 1H, H_G), 6.23 (d, J = 8.0 Hz, 1H, H_F), 4.12 (m, 2H, H_H). ESI-MS (M^+ = 700.1412).

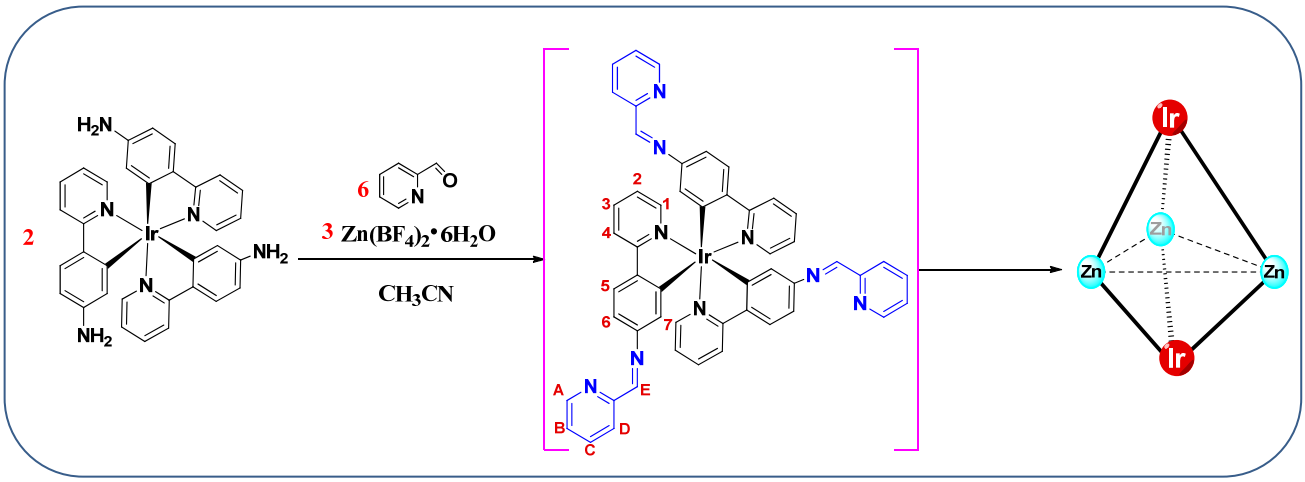

2.2. Synthesis of compound Ir-Zn1

To a Schlenk tube was added *fac*-Ir-NH_2 (35 mg, 0.05 mmol, 2 equiv.), 2-formylpyridine (15 μL, 0.15 mmol, 6 equiv.), $Zn(BF_4)_2\cdot 6H_2O$ (25 mg, 0.075 mmol, 3 equiv.) in acetonitrile (40 mL). The solution was refluxed for 24 h under the protection of N_2. Then the solution was placed in a sealed tank full of N_2 and diffused with diethyl ether then the dark wine crystals was obtained (yield 90%, based on the crytsal dried vaccum). ^{1}H NMR ($C_2D_2Cl_4$-d_2, ppm): δ 7.54 (m, 1H, H_E), 8.59 (m, 1H, H_C), 8.34 (d, J = 8.0 Hz, 1H, H_A), 7.77 (t, 1H, J = 8.0 Hz, H_B), 7.58 (m, 1H, H_D), 7.53-7.45 (m, 3H, $H_{1,3,4}$), 7.17-7.01 (m, 3H, $H_{2,5,7}$), 6.8 (m, 1H, H_6). ESI-MS m/z = 541.5710 $[Zn_3(Ir\text{-}PY)_2\cdot OH^-\cdot F^-]^{4+}$, 751.1100 $[Zn_3(Ir\text{-}PY)_2\cdot OH^-\cdot F^-\cdot BF_4^-]^{3+}$ and 1170.1512 $[Zn_3(Ir\text{-}PY)_2\cdot OH^-\cdot F^-\cdot 2BF_4^-]^{2+}$. Anal. Calc. for $[Zn_3(C_{51}H_{36}N_9Ir)_2(OH)(F)(H_2O)]$ $(BF_4)_4\cdot H_2O$: H, 3.04; C, 48.05; N, 9.89. Found: H, 2.95; C, 48.08; N, 10.06.

2.3. Synthesis of compound Ir-Zn2

This complex was synthesized following the same procedure as described for compound **Ir-Zn1**, the solution was exposed on air over one week or placed in a sealed tank full of CO_2 and then diffused with diethyl ether, the dark wine crystals were obtained (yield 92%, based on the crytsal dried vaccum). ^{1}H NMR ($C_2D_2Cl_4$-d_2, ppm): δ 9.39 (m, 1H, H_E), 8.48 (m, 1H, H_C), 8.26 (d, J = 8.0 Hz, 1H, H_A), 7.90 (m, 1H, H_B), 7.69 (m, 1H, H_D), 7.51-7.46 (m, 3H, $H_{1,3,4}$), 7.16-7.04 (m, 3H, $H_{2,5,7}$), 6.81-6.69 (m, 1H, H_6). ESI-MS: $[Zn_3(Ir–\mathbf{PY})_2·CO_3^{2-}]^{4+}$ 547.6038, $[Zn_3(Ir–\mathbf{PY})_2·CO_3^{2-}·BF_4^-]^{3+}$ 759.1555, $[Zn_3(Ir–\mathbf{PY})_2·CO_3^{2-}·2BF_4^-]^{2+}$ 1182.2535. Anal. Calc. for $[Zn_3(C_{51}H_{36}N_9Ir)_2·CO_3](BF_4)_4·(H_2O)$: H, 2.92; C, 48.41; N, 9.87. Found: H, 2.99; C, 47.83; N, 9.73.

2.4. Synthesis of compound Ir-Zn2'

Control experiments using a labeled $^{13}CO_2$ source to synthesise compound **Ir-Zn2'**. An amount of Cage **1** (30 mg, 0.01 mmol) was dissolved in CH_3CN (100 mL) under N_2 in a septum-sealed Schlenk flask, and excess $^{13}CO_2$ was injected by gas-tight syringe. Then the mixed solution was placed in a sealed tank full of $^{13}CO_2$ and crystals of compound **Ir-Zn2'** were obtained over one week (yield 86%, based on the crytsal dried vaccum). ESI-MS: $[Zn_3(Ir–\mathbf{PY})_2·^{13}CO_3^{2-}]^{4+}$ 547.8039, $[Zn_3(Ir–\mathbf{PY})_2·^{13}CO_3^{2-}·BF_4^-]^{3+}$ 759.4199, $[Zn_3(Ir–\mathbf{PY})_2·^{13}CO_3^{2-}·2BF_4^-]^{2+}$ 1182.5814.

2.5. Synthesis of compound Ir-Zn3

To a Schlenk tube was added *fac*-Ir-NH_2 (35 mg, 0.05 mmol, 2 equiv.), 2-formylpyridine (15 μL, 0.15 mmol, 6 equiv.), $Zn(BF_4)_2·6H_2O$ (25 mg, 0.075 mmol, 3 equiv.) in acetonitrile (40 mL). The solution was refluxed for 24 h under the protection of N_2. A 6% solution of sulphur dioxide in water (266 μL, 0.25 mmol, 10 eq.) was added dropwise to the solution of **Ir-Zn1** with 0.25 mmol triethylamine. The mixture was stirred at room tempreature overnight. Then the solution was diffused with diethyl ether then the wine red crystals was obtained (yield 91%, based on the crytsal dried vaccum). ^{1}H NMR ($C_2D_2Cl_4$-d_2, ppm): δ 9.41 (d, J = 8.0 Hz, 1H), 8.57 (dd, J = 12.0, 8.0 Hz, 1H), 8.39 (dd, J = 12.0, 8.0 Hz, 1H), 7.86 (m, 1H), 7.65 ((m, 1H), 7.36 (m, 1H), 7.18 (m, 1H), 6.69 (m, 1H). ESI-MS: $[Zn_3(Ir–\mathbf{PY})_2·SO_3^{2-}]^{4+}$ 552.5938, $[Zn_3(Ir–\mathbf{PY})_2·SO_3^{2-}·BF_4^-]^{3+}$ 765.7897, $[Zn_3(Ir–\mathbf{PY})_2·SO_3^{2-}·2BF_4^-]^{2+}$ 1192.1641. Anal. Calc. for $[Zn_3(C_{51}H_{36}N_9Ir)_2·SO_3](BF_4)_4·(H_2O)$: H, 2.95; C, 47.23; N, 9.72. Found: H, 2.87; C, 47.68; N, 9.79.

2.6 ESI-MS spectra of the compound Ir-Zn1.

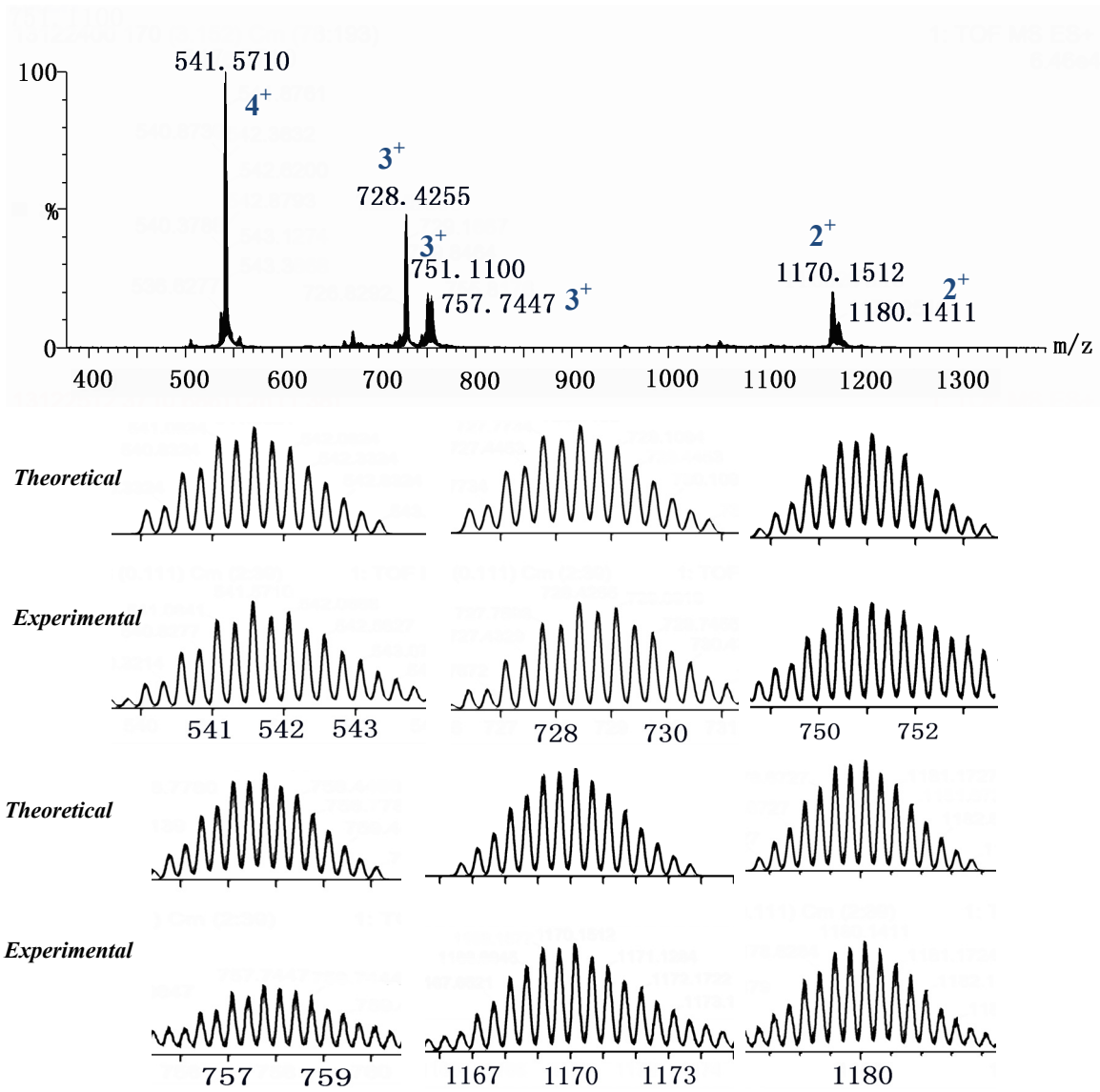

Peak number	Ex-Value	Th-Value	Specie Assigned
1	541.5710	541.5824	$[Zn_3(Ir\text{-}PY)_2 \cdot OH^- \cdot F^-]^{4+}$
2	728.4255	728.4455	$[Zn_3(Ir\text{-}PY)_2 \cdot OH^- \cdot 2F^-]^{3+}$
3	751.1100	751.1093	$[Zn_3(Ir\text{-}PY)_2 \cdot OH^- \cdot F^- \cdot BF_4^-]^{3+}$
4	757.7447	757.7780	$[Zn_3(Ir\text{-}PY)_2 \cdot H_2O \cdot 2F^- \cdot BF_4^-]^{3+}$
5	1170.1512	1170.1696	$[Zn_3(Ir\text{-}PY)_2 \cdot OH^- \cdot F^- \cdot 2BF_4^-]^{2+}$
6	1180.1411	1180.1727	$[Zn_3(Ir\text{-}PY)_2 \cdot H_2O \cdot 2F^- \cdot 2BF_4^-]^{2+}$

Figure S1 ESI-MS spectra of compound **Ir-Zn1** in acetonitrile

2.7 ESI-MS spectra of the compound Ir-Zn2.

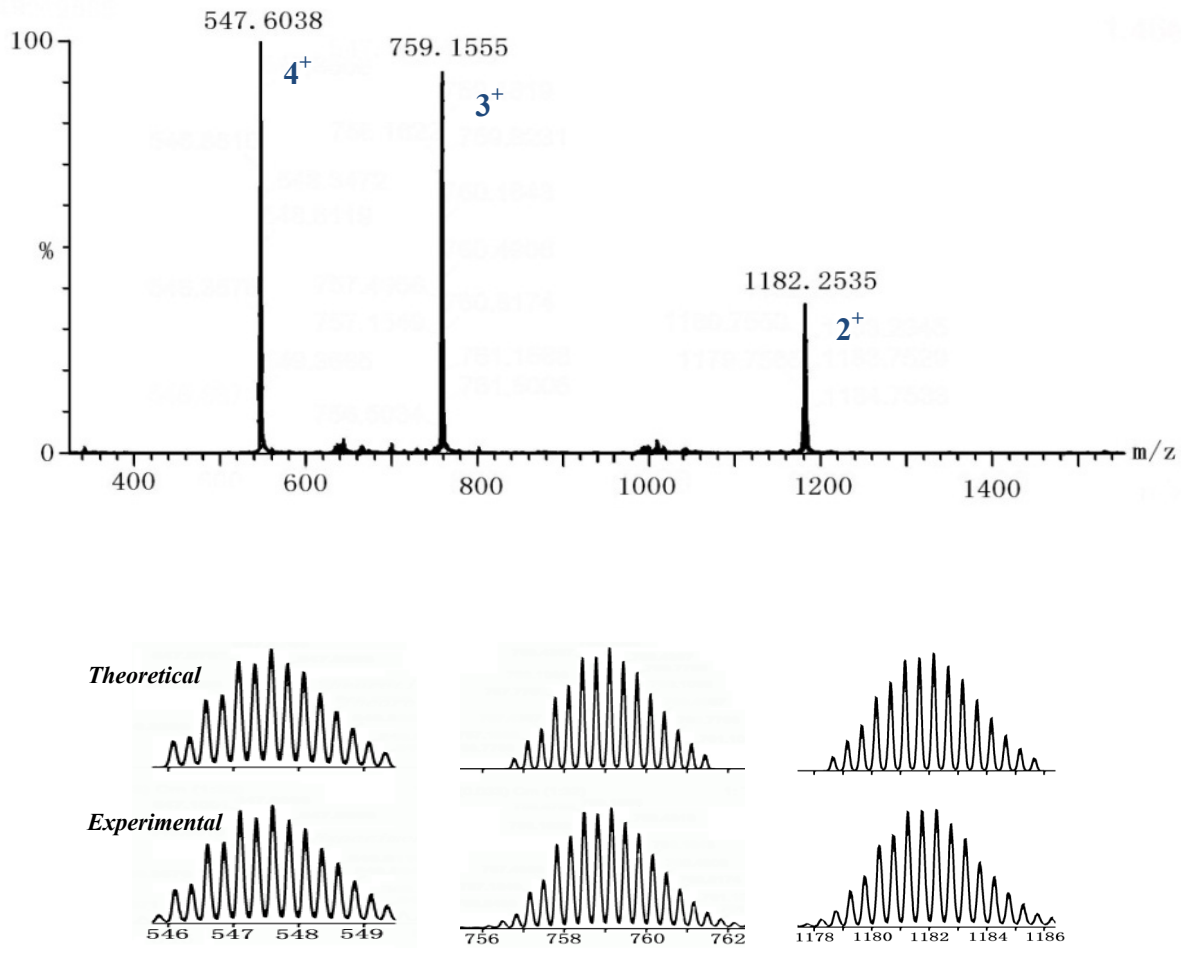

Peak number	Ex-Value	Th-Value	Specie Assigned
1	547.6038	547.5783	$[Zn_3(Ir–\mathbf{PY})_2⊃CO_3^{2-}]^{4+}$
2	759.1555	759.1038	$[Zn_3(Ir–\mathbf{PY})_2⊃CO_3^{2-}·BF_4^-]^{3+}$
3	1182.2535	1182.1614	$[Zn_3(Ir–\mathbf{PY})_2⊃CO_3^{2-}·2BF_4^-]^{2+}$

Figure S2 ESI-MS spectra of compound **Ir-Zn2** in acetonitrile

2.8 ^{13}C NMR spectra of the compound Ir-Zn1 and Ir-Zn2.

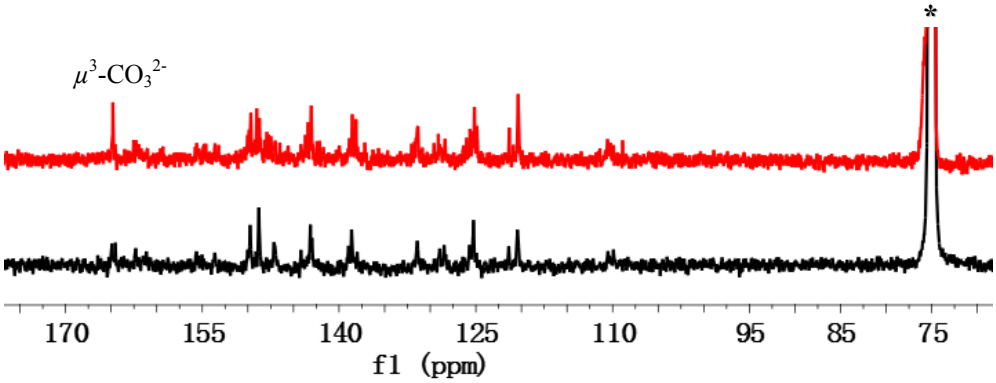

Figure S3 ^{13}C NMR of compound **Ir-Zn2** (red) and compound **Ir-Zn1** (black), showing the presence of a peak at 164.0 ppm for CO_3^{2-}. (Solvent $C_2D_2Cl_4$ signals were marked using *)

2.9 ^{13}C NMR spectra of the compound Ir-Zn2'

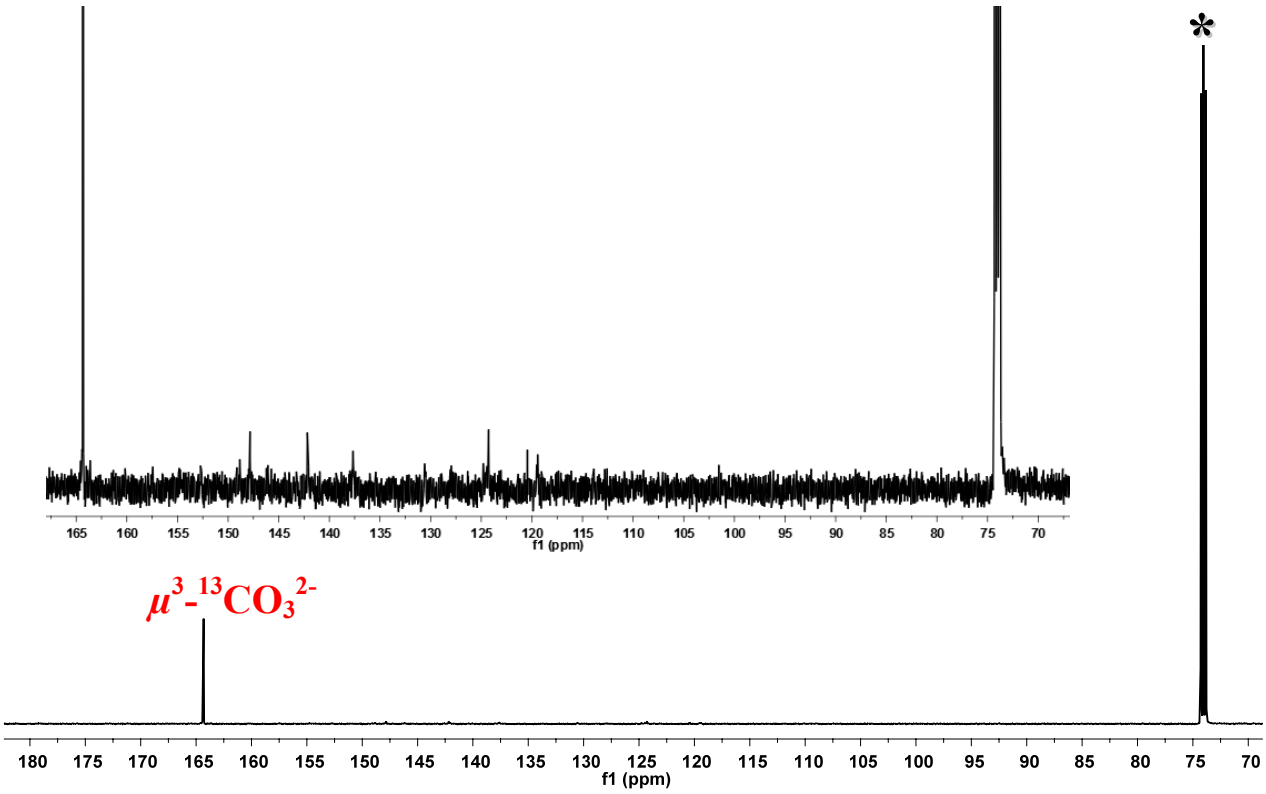

Figure S4 ^{13}C NMR of compound **Ir-Zn2',** showing the presence of a peak at 164.0 ppm for $^{13}CO_3^{2-}$. (Solvent $C_2D_2Cl_4$ signals were marked using *).

2.10 ESI-MS spectra of the compound Ir-Zn2'.

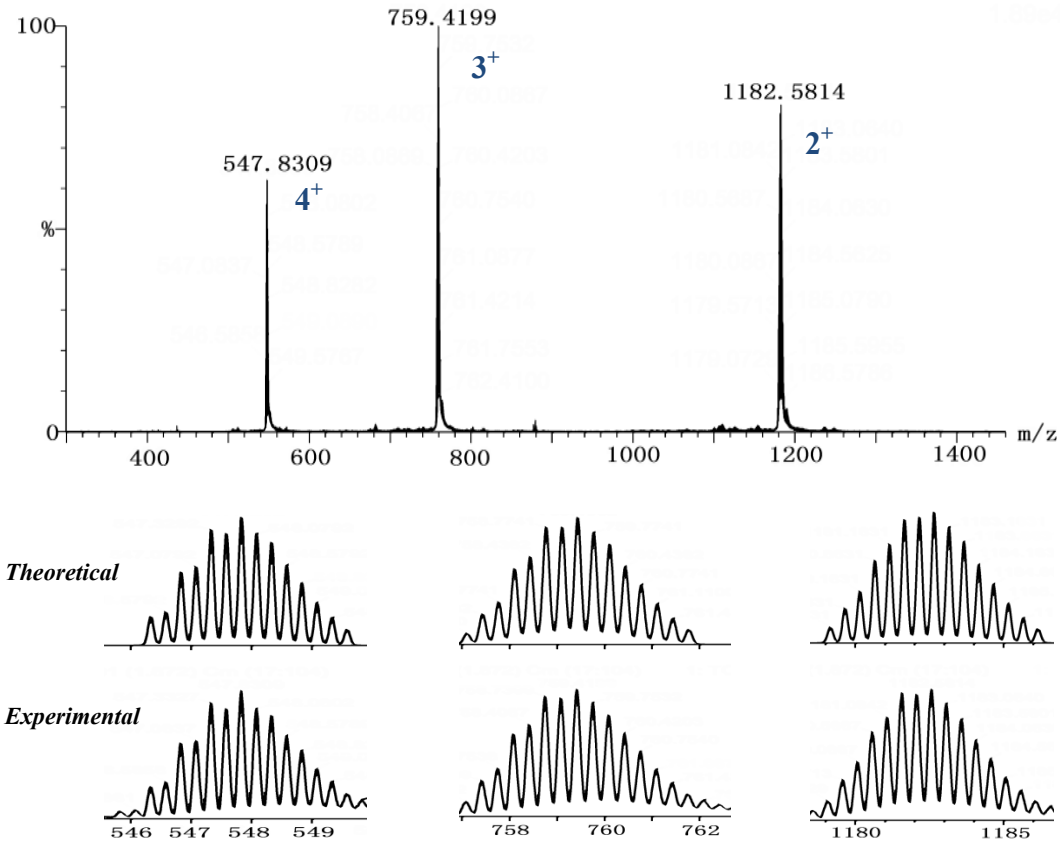

Peak number	Ex-Value	Th-Value	Specie Assigned
1	547.8309	547.8292	$[Zn_3(Ir–\mathbf{PY})_2\supset{}^{13}CO_3^{2-}]^{4+}$
2	759.4199	759.4382	$[Zn_3(Ir–\mathbf{PY})_2\supset{}^{13}CO_3^{2-}\cdot BF_4^-]^{3+}$
3	1182.5814	1182.6631	$[Zn_3(Ir–\mathbf{PY})_2\supset{}^{13}CO_3^{2-}\cdot 2BF_4^-]^{2+}$

Figure S5 ESI-MS spectra of compound **Ir-Zn2'** in acetonitrile.

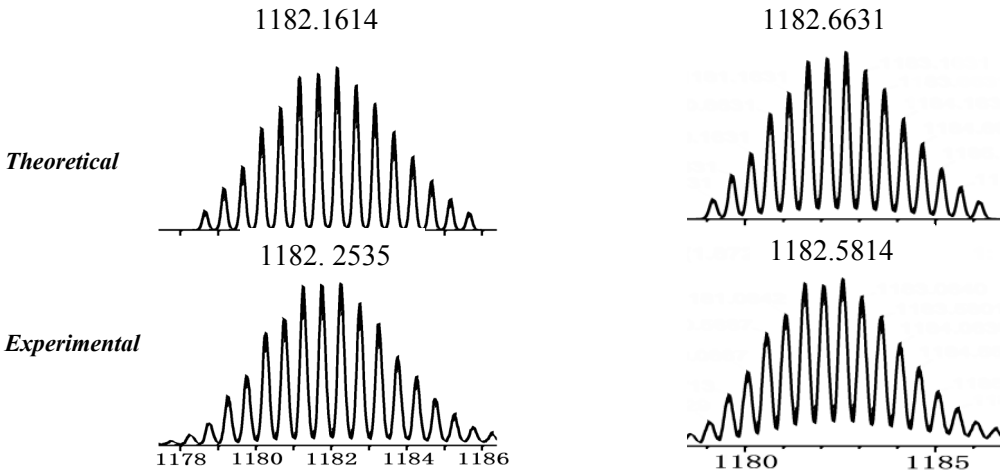

$[Zn_3(Ir–\mathbf{PY})_2 \supset \mathbf{CO_3^{2-}} \cdot 2BF_4^-]^{2+}$ $[Zn_3(Ir–\mathbf{PY})_2 \supset \mathbf{^{13}CO_3^{2-}} \cdot 2BF_4^-]^{2+}$

Figure S6 The simulation results obtained on the basis of natural isotopic abundance for $[Zn_3(Ir–PY)_2 \supset CO_3^{2-} \cdot 2BF_4^-]^{2+}$ and $[Zn_3(Ir–PY)_2 \supset {}^{13}CO_3^{2-} \cdot 2BF_4^-]^{2+}$, respectively.

2.11 ESI-MS spectra of the compound Ir-Zn3

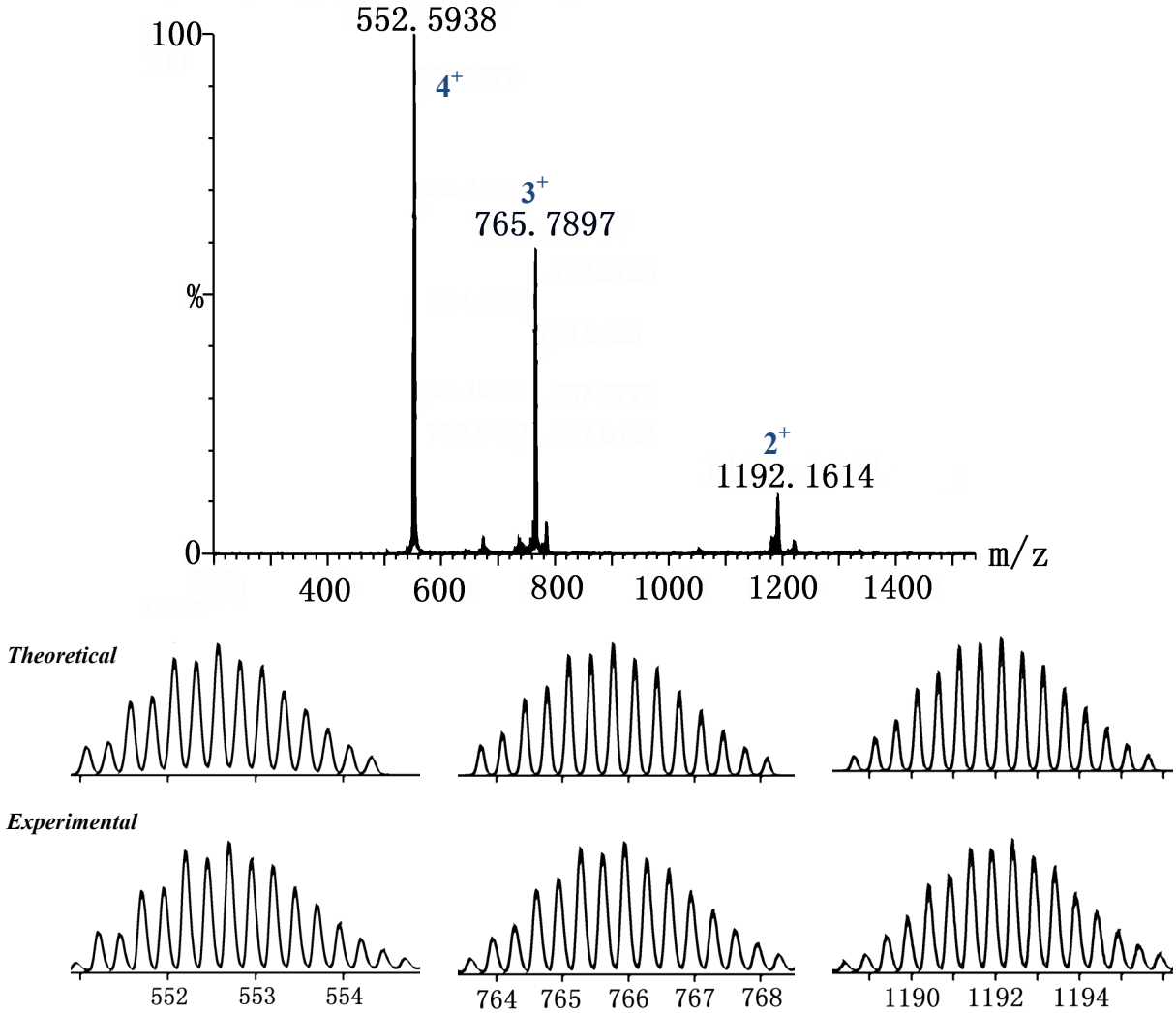

Peak number	Ex-Value	Th-Value	Specie Assigned
1	552.5938	552.5714	$[Zn_3(Ir–\mathbf{PY})_2 \supset SO_3^{2-}]^{4+}$
2	765.7897	765.7658	$[Zn_3(Ir–\mathbf{PY})_2 \supset SO_3^{2-} \cdot BF_4^-]^{3+}$
3	1192.1614	1192.1475	$[Zn_3(Ir–\mathbf{PY})_2 \supset SO_3^{2-} \cdot 2BF_4^-]^{2+}$

Figure S7 ESI-MS spectra of compound **Ir-Zn3** in acetonitrile.

3. Single Crystal Analyses of the Complexes.

3.1 Crystallography

Intensities of the crystal data were collected on a Bruker SMART APEX CCD diffractometer with graphite monochromated Mo-Kα (λ = 0.71073 Å) using the SMART and SAINT programs.[S2] The structures were solved by direct methods and refined on *F2* by full-matrix least-squaresmethods with SHELXTL *version* 5.1.[S3] Crystallographic data have been deposited with the CCDC number being 1001631, 1001629 and 1442696.

For the crystal data of compound **Ir-Zn1**, six cabon atoms in one of the imine-pyridine moiety on the ligand backbone were disordered into two parts with the site occupancy factors (s.o.f.) of each parts being fixed as 0.5, respectively. The The coordinated fluoride atom on one zinc center was disordered into two parts with the s.o.f. of each part being fixed as 0.67 and 0.33, respectively. Totally seven fluoride atoms in two BF_4^- anioins were disordered into two parts with the s.o.f. of each parts being refined with free variables. Except the disordered parts and the partly occupied solvent molecules, the other non-hydrogen atoms were refined anisotropically. Hydrogen atoms within the ligand backbones and the solvent acetonitrile molecules were fixed geometrically at calculated distances and allowed to ride on the parent non-hydrogen atoms. The distances of the B-F bond in each anion were restrained to be same. Thermal parameters on adjacent atoms of the disordered carbon atoms and the disordered BF_4^- groups were restrained to be similar. CCDC 1001631.

For the crystal data of compound **Ir-Zn2**, the non-hydrogen atoms in the backbone of the cage complex were refined anisotropically. Hydrogen atoms within the ligand backbones and the solvent molecules were fixed geometrically at calculated distances and allowed to ride on the parent non-hydrogen atoms. The three oxygen atoms of the carbonate ion were disordered into two parts with the s.o.f. of each parts being refined with free variables. Three of the four fluoride atoms in one BF_4^- anioins were disordered into two parts with the s.o.f. of each parts being fixed as 0.5, respectively. Thermal parameters on adjacent atoms of the disordered BF_4^- groups were restrained to be similar. CCDC 1001629.

For the crystal data of compound **Ir-Zn3**, except the partly occupied solvent molecules, the non-hydrogen atoms were refined anisotropically. Hydrogen atoms within the ligand backbones and the solvent molecules were fixed geometrically at calculated distances and allowed to ride on the parent non-hydrogen atoms. The SO_3^{2-} ion was diorered into two parts with the s.o.f. of each part being fiexed as 0.5. Some distances of the solvent molecules were restrained as ideal geometry. Thermal parameters on adjacent atoms of the solvent molecules were restrained to be similar. CCDC 1442696.

	Ir-Zn1	**Ir-Zn2**	**Ir-Zn3**
Formula	$Ir_2Zn_3C_{116}H_{98}N_{25}O_3B_4F_{17}$	$Ir_2Zn_3C_{123}H_{116}N_{22}O_7B_4F_{16}$	$Ir_2Zn_3C_{1118}H_{104}N_{24}O_6B_4F_{16}S$
V(Å^3)	2836.94	2942.13	2914.06
T/K	200(2)	200(2)	200(2)
Crystal system	Monoclinic	Monoclinic	Monoclinic
Space group	P2(1)/c	P2(1)/c	P2(1)/c
a/Å	29.505(1)	29.010(1)	29.347(3)
b/Å	19.110(1)	19.025(1)	18.872(1)
c/Å	24.976(1)	24.810(1)	25.160(2)
β (º)	112.295(2)	111.60(1)	112.374(5)
V/Å^3	13029.4(7)	12729.9(4)	12885.5(19)
Z	4	4	4
D_c/g cm^{-1}	1.446	1.535	1.502
μ/mm^{-1}	2.661	2.727	2.708
F(000)	5640	5888	5808
No.refsmeasued	69914	102609	78788
No. unique refs	22924	22417	22661
R_{int}	0.0530	0.0754	0.1099
$R_1[I > 2\sigma(I)]$	0.0749	0.0520	0.0737
wR_2 (all data)	0.2446	0.1648	0.2030
Goodness of Fit	1.019	1.026	1.012
CCDC No.	**1001631**	**1001629**	**1442696**

$R_1 = \sum \| F_o | - | F_c \| / | \sum | F_o | .wR_2 = [\sum w(F_o^2 - F_c^2)_2 / \sum (F_o)^2]$ ½

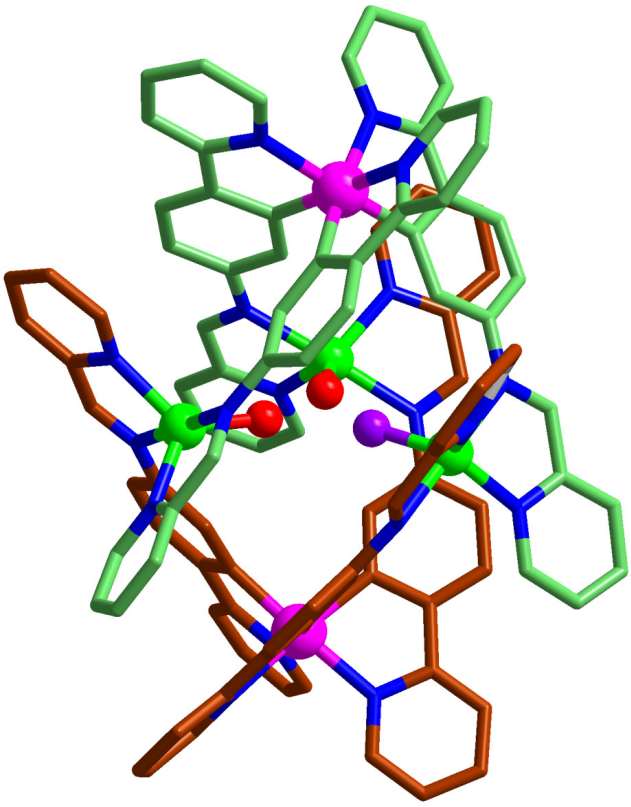

Ir-Zn1

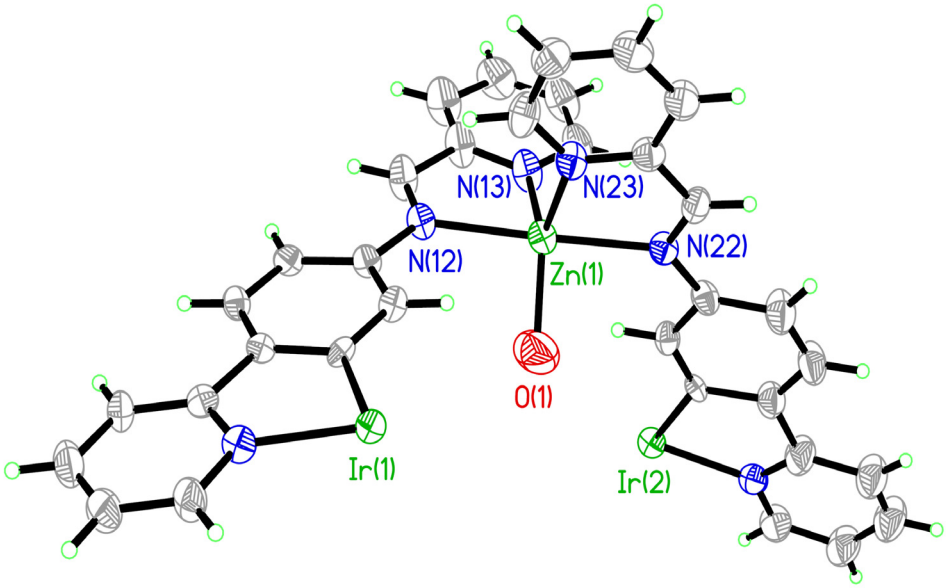

Figure S8 Coordination geometry of the Zn(1) atom in **Ir-Zn1**. Selected bond distances (Å) and angles (°): Zn(1)−N(12) 2.174(3), Zn(1)−N(13) 2.037(3), Zn(1)−N(22) 2.169(3), Zn(1)−N(23) 2.057(3), Zn(1)−O(1) 1.863(4); O(1)−Zn(1)−N(13) 126.40(15), O(1)−Zn(1)−N(23) 122.42(15), O(1)−Zn(1)−N(22) 88.72(18), O(1)−Zn(1)−N(12) 93.16(18), N(13)−Zn(1)−N(23) 111.16(14), N(13)−Zn(1)−N(22) 100.20(13), N(13)−Zn(1)−N(12) 78.72(13), N(23)−Zn(1)−N(22) 79.39(12), N(23)−Zn(1)−N(12) 99.56(12), N(22)−Zn(1)−N(12) 178.12(12).

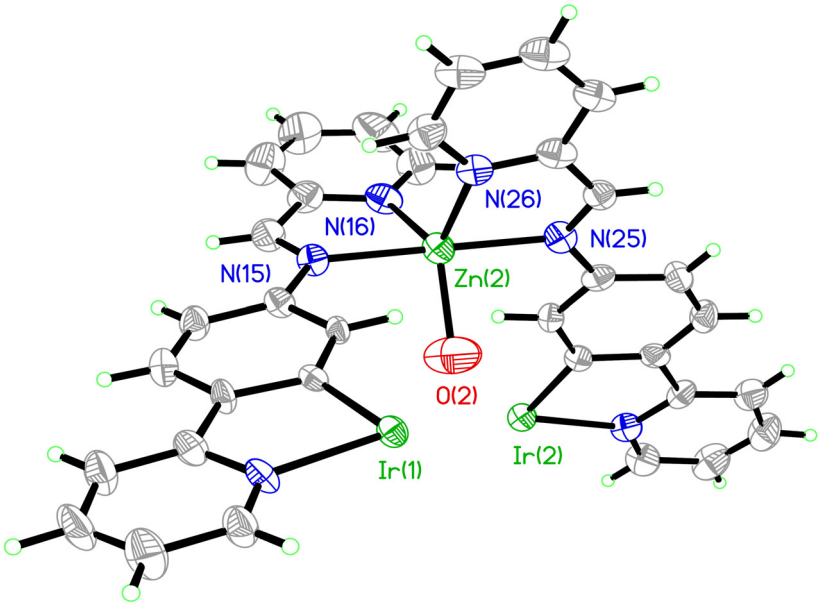

Figure S9 Coordination geometry of the Zn(2) atom in **Ir-Zn1**. Selected bond distances (Å) and angles (°): Zn(2)−N(15) 2.159(3), Zn(2)−N(16) 2.039(3), Zn(2)−N(25) 2.133(3), Zn(2)−N(26) 2.039(4), Zn(2)−O(2) 1.921(5); O(2)−Zn(2)−N(16) 124.07(18), O(2)−Zn(2)−N(26) 124.33(17), O(2)−Zn(2)−N(25) 89.46(16), O(2)−Zn(2)−N(15) 90.07(16), N(26)−Zn(2)−N(16) 111.56(14), N(26)−Zn(2)−N(25) 79.96(14), N(26)−Zn(2)−N(15) 98.44(13), N(16)−Zn(2)−N(25) 102.91(12), N(16)−Zn(2)−N(15) 79.24(12), N(25)−Zn(2)−N(15) 177.66(12).

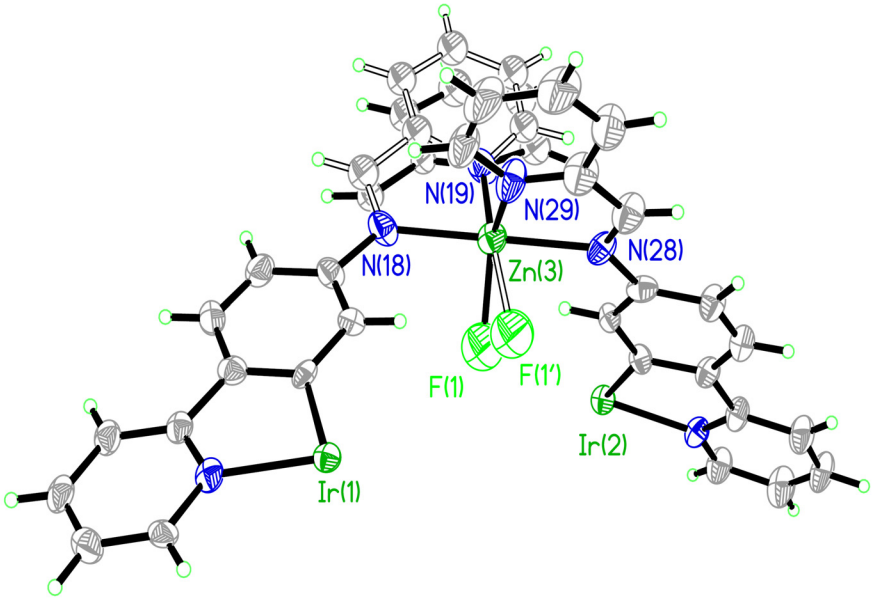

Figure S10 Coordination geometry of the Zn(3) atom in **Ir-Zn1**. Selected bond distances (Å) and angles (°): Zn(3)−N(18) 2.133(3), Zn(3)−N(19) 2.032(4), Zn(3)−N(28) 2.153(3), Zn(3)−N(29) 2.030(4), Zn(3)−F(1) 1.888(6), Zn(3)−F(1') 1.882(14); F(1)−Zn(3)−N(19) 122.3(2), F(1)−Zn(3)−N(29) 124.6(2), F(1)−Zn(3)−N(18) 88.0(2), F(1)−Zn3−N(28) 91.9(2), F(1')−Zn(3)−F(1) 39.9(4), F(1')−Zn(3)−N(19) 158.8(3), F(1')−Zn(3)−N(29) 86.2(4), F(1')−Zn(3)−N(18) 105.7(4), F(1')−Zn(3)−N(28) 73.9(4), N(19)−Zn(3)−N(29) 113.06(16), N(19)−Zn(3)−N(18) 80.86(14), N(19)−Zn(3)−N(28) 99.67(14), N(29)−Zn(3)−N(18) 99.11(13), N(29)−Zn(3)−N(28) 80.48(13), N(18)−Zn(3)−N(28) 179.42(14).

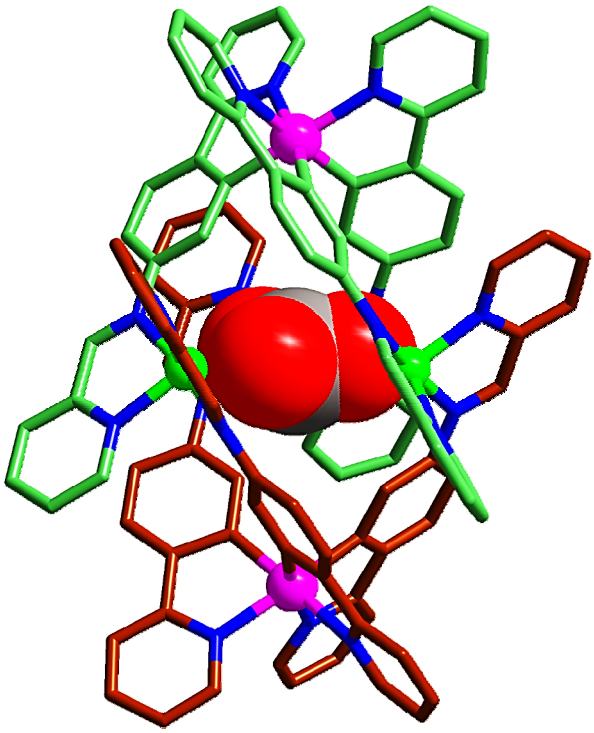

Ir-Zn1⊃CO_3^{2-}

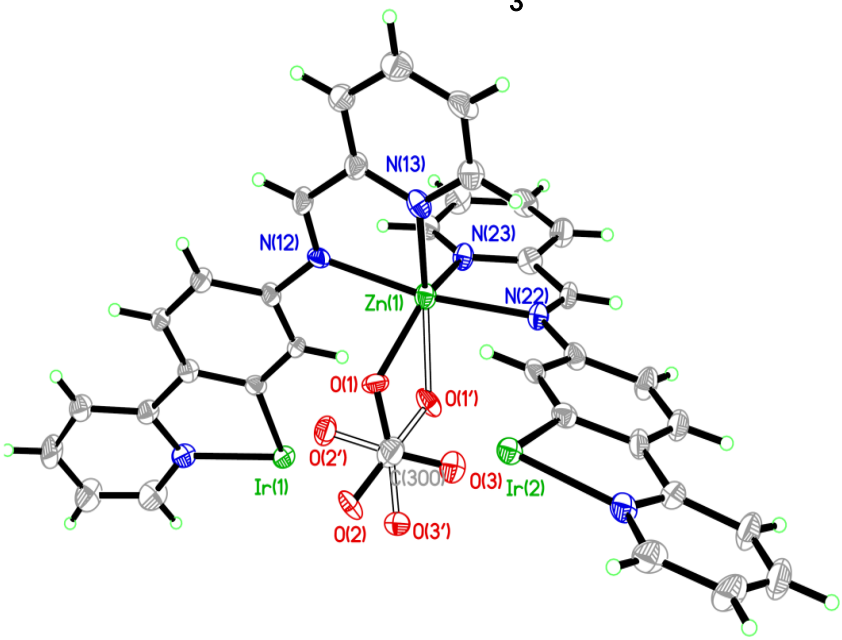

Figure S11 Coordination geometry of the Zn(1) atom in **Ir-Zn2**. Selected bond distances (Å) and angles (°): Zn(1)−N(12) 2.197(6), Zn(1)−N(13) 2.069(6), Zn(1)−N(22) 2.186(6), Zn(1)−N(23) 2.082(6), Zn(1)−O(1) 1.952(8), Zn(1)−O(1') 1.931(16); O(1)−Zn(1)−N(13) 111.2(3), O(1)−Zn(1)−N(23) 140.7(3), O(1)−Zn(1)−N(22) 107.8(3), O(1)−Zn(1)−N(12) 81.7(3), N(13)−Zn(1)−N(12) 77.7(2), N(13)−Zn(1)−N(22) 97.0(2), N(13)−Zn(1)−N(23) 106.3(2), N(23)−Zn(1)−N(22) 78.2(2), N(23)−Zn(1)−N(12) 95.5(2), N(22)−Zn(1)−N(12) 170.4(2), O(1')−Zn(1)−O(1) 40.9(5), O(1')−Zn(1)−N(13) 144.6(4), O(1')−Zn(1)−N(23) 107.1(5), O(1')−Zn(1)−N(22) 79.0(5), O(1')−Zn(1)−N(12) 110.0(4).

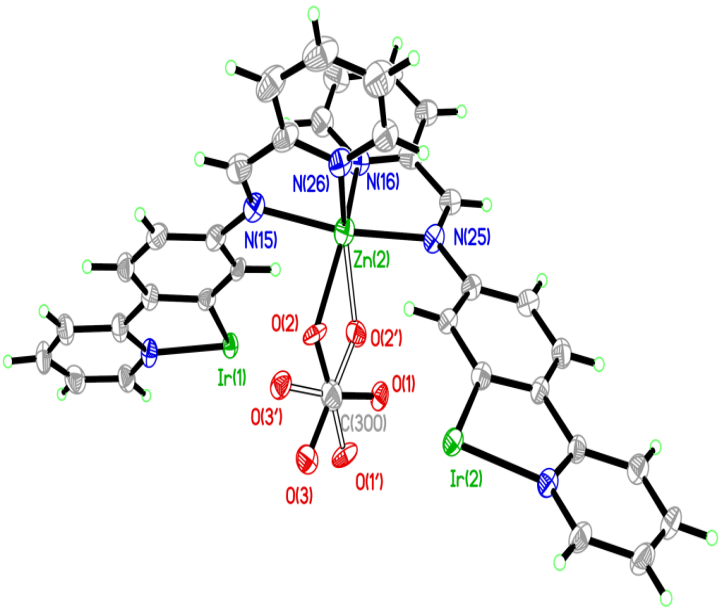

Figure S12 Coordination geometry of the Zn(2) atom in **Ir-Zn2**. Selected bond distances (Å) and angles (°): Zn(2)−N(15) 2.176(6), Zn(2)−N(16) 2.075(6), Zn(2)−N(25) 2.140(6), Zn(2)−N(26) 2.077(7), Zn(2)−O(2) 1.951(9), Zn(2)−O(2') 1.966(17); O(2)−Zn(2)−N(16) 110.7(3), O(2)−Zn(2)−N(26) 139.1(3), O(2)−Zn(2)−N(25) 108.4(3), O(2)−Zn(2)−N(15) 79.6(3), N(26)−Zn(2)−N(16) 107.7(3), N(26)−Zn(2)−N(25) 78.7(3), N(26)−Zn(2)−N(15) 94.8(2), N(16)−Zn(2)−N(25) 98.6(2), N(16)−Zn(2)−N(15) 78.7(2), N(25)−Zn(2)−N(15) 172.0(2), O(2')−Zn(2)−O(2) 42.2(5), O(2')−Zn(2)−N(16) 144.0(5), O(2')−Zn(2)−N(26) 106.3(5), O(2')−Zn(2)−N(25) 76.7(5), O(2')−Zn(2)−N(15) 110.0(5).

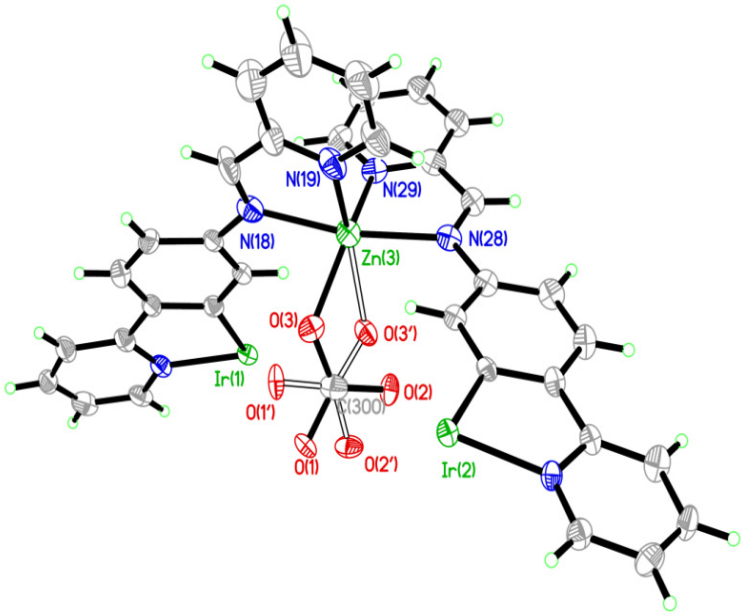

Figure S13 Coordination geometry of the Zn(3) atom in **Ir-Zn2**. Selected bond distances (Å) and angles (°): Zn(3)−N(18) 2.194(7), Zn(3)−N(19) 2.072(7), Zn(3)−N(28) 2.168(6), Zn(3)−N(29) 2.099(6), Zn(3)−O(3) 1.985(9), Zn(3)−O(3') 1.996(17); O(3)−Zn(3)−N(19) 109.7(3), O(3)−Zn(3)−N(29) 140.5(3), O(3)−Zn(3)−N(18) 79.4(3), O(3)−Zn(3)−N(28) 110.6(3), N(19)−Zn(3)−N(29) 106.8(3), N(19)−Zn(3)−N(18) 78.3(3), N(19)−Zn(3)−N(28) 97.3(3), N(29)−Zn(3)−N(18) 93.9(3), N(29)−Zn(3)−N(28) 78.7(2), N(18)−Zn(3)−N(28) 170.0(2), O(3')−Zn(3)−O(3) 43.4(5), O(3')−Zn(3)−N(19) 143.7(5), O(3')−Zn(3)−N(29) 107.4(4), O(3')−Zn(3)−N(18) 110.8(5), O(3')−Zn(3)−N(28) 78.1(5).

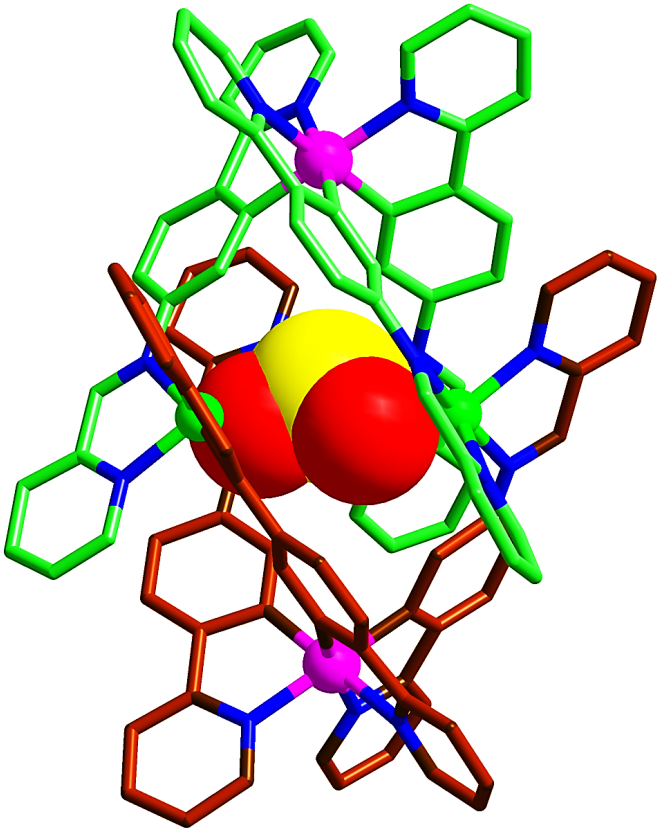

Ir-Zn1⊃SO_3^{2-}

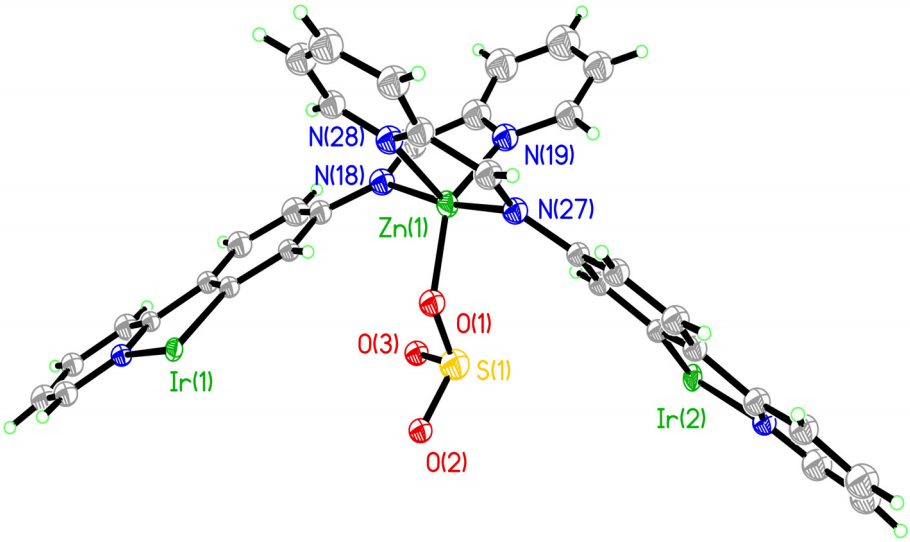

Figure S14 Coordination geometry of the Zn(1) atom in **Ir-Zn3**. Selected bond distances (Å) and angles (°): Zn(1)-O(1) 1.930(9), Zn(1)-N(19) 2.061(6), Zn(1)-N(28) 2.074(5), Zn(1)-N(27) 2.180(5), Zn(1)-N(18) 2.189(5); O(1)-Zn(1)-N(19) 145.8(3), O(1)-Zn(1)-N(28) 105.5(3), N(19)-Zn(1)-N(28) 107.6(2), N(19)-Zn(1)-N(27) 97.41(19), N(28)-Zn(1)-N(27) 78.94(17), O(1)-Zn(1)-N(18) 106.5(3), (19)-Zn(1)-N(18) 79.1(2), N(28)-Zn(1)-N(18) 95.00(18), N(27)-Zn(1)-N(18) 171.87(19).

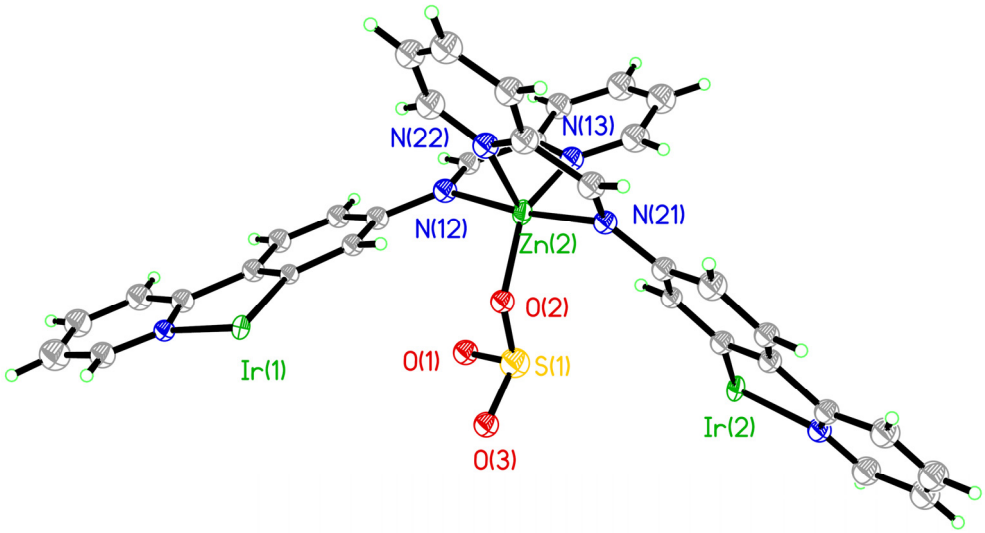

Figure S15 Coordination geometry of the Zn(2) atom in **Ir-Zn3**. Selected bond distances (Å) and angles (°): Zn(2)-O(2) 1.905(8), Zn(2)-N(13) 2.049(4), Zn(2)-N(22) 2.055(6), Zn(2)-N(21) 2.173(4), Zn(2)-N(12) 2.177(4); O(2)-Zn(2)-N(13) 145.9(3), O(2)-Zn(2)-N(22) 104.5(3), N(13)-Zn(2)-N(22) 108.6(2), O(2)-Zn(2)-N(21) 79.5(2), N(13)-Zn(2)-N(21) 98.87(17), N(22)-Zn(2)-N(21) 78.89(19), O(2)-Zn(2)-N(12) 105.2(2), N(13)-Zn(2)-N(12) 79.41(16), N(22)-Zn(2)-N(12) 96.22(19), N(21)-Zn(2)-N(12) 174.1(2).

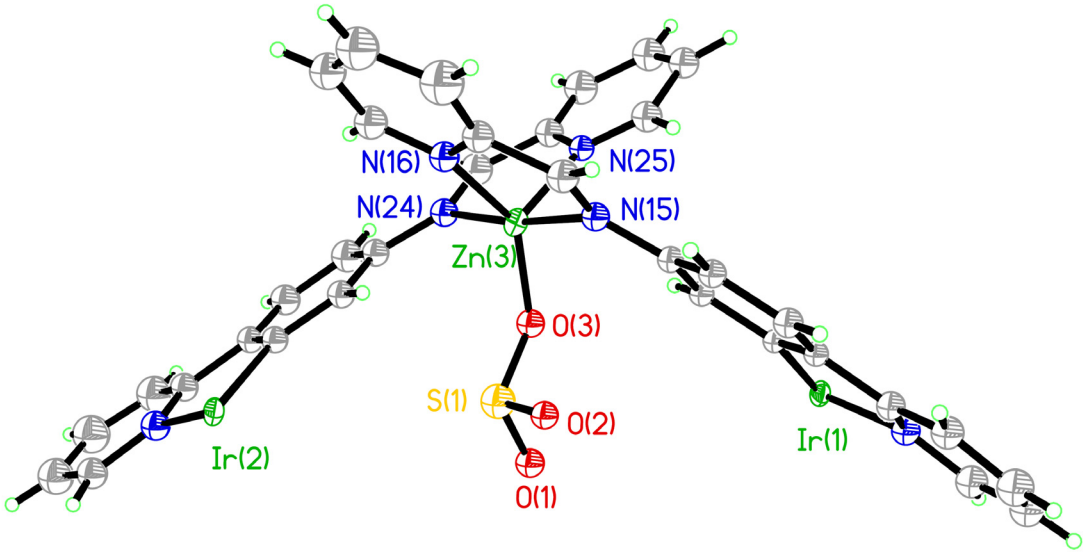

Figure S16 Coordination geometry of the Zn(3) atom in **Ir-Zn3**. Selected bond distances (Å) and angles (°): Zn(3)-O(3) 1.859(8), Zn(3)-N(16) 2.055(5), Zn(3)-N(25) 2.064(4), Zn(3)-N(15) 2.187(5), Zn(3)-N(24) 2.192(5); O(3)-Zn(3)-N(16) 144.8(3), O(3)-Zn(3)-N(25) 104.7(3), N(16)-Zn(3)-N(25) 109.01(19), O(3)-Zn(3)-N(15) 107.6(3), N(16)-Zn(3)-N(15) 78.24(19), N(25)-Zn(3)-N(15) 7.25(19), O(3)-Zn(3)-N(24) 78.7(3), N(16)-Zn(3)-N(24) 98.2(2), N(25)-Zn(3)-N(24) 78.29(19), N(15)-Zn(3)-N(24) 173.17(18).

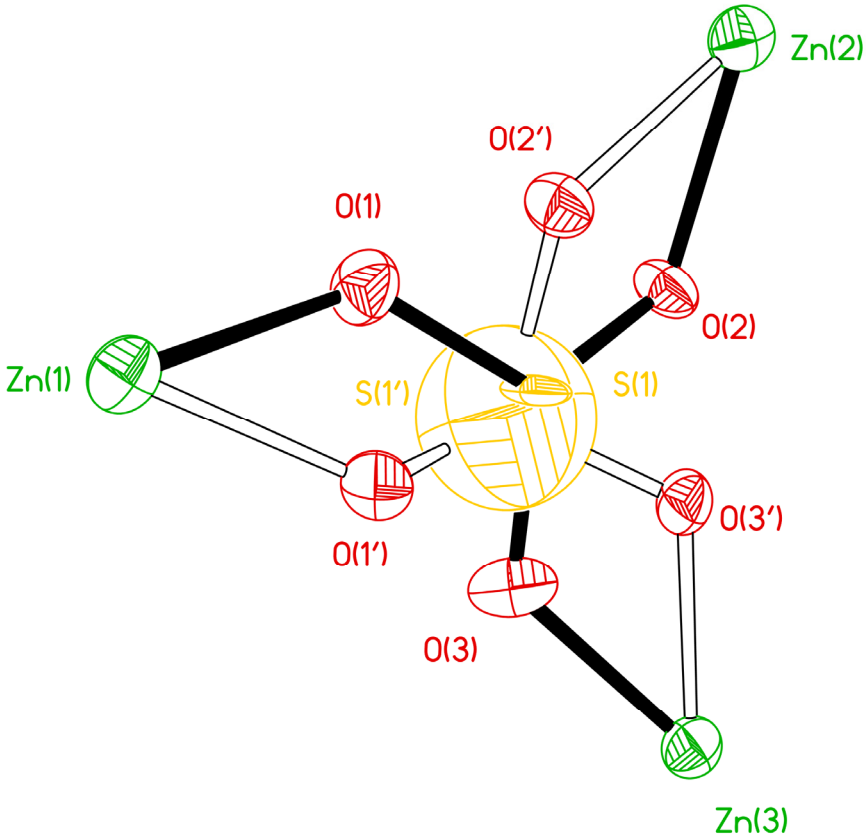

Figure S17 Coordination geometry of the SO_3^{2-} in **Ir-Zn3**. Selected bond distances (Å) and angles (°): S(1)-O(1) 1.427(8), S(1)-O(2) 1.449(9), S(1)-O(3) 1.491(9), S(1')-O(1') 1.384(19), S(1')-O(3') 1.416(16), S(1')-O(2') 1.642(16); O(1)-S(1)-O(2) 114.0(5), O(1)-S(1)-O(3) 116.7(5), O(2)-S(1)-O(3) 114.7(5), S(1)-O(1)-Zn(1) 127.8(6), S(1)-O(2)-Zn(2) 126.4(5), S(1)-O(3)-Zn(3) 128.3(5), O(1')-S(1')-O(3') 117.3(12), O(1')-S(1')-O(2') 101.6(10), O(3')-S(1')-O(2') 101.6(9), S(1')-O(1')-Zn(1) 130.1(8), S(1')-O(2')-Zn(2) 126.4(8), S(1')-O(3')-Zn(3) 117.7(8).

4. Luminescence Spectra of the Compounds and the Tracing of the Transformation

4.1 Luminescence spectra of Ir-Zn1 and Ir-Zn2 (1.0×10^{-5} M in deaerated acetonitrile solution, excited at 360nm).

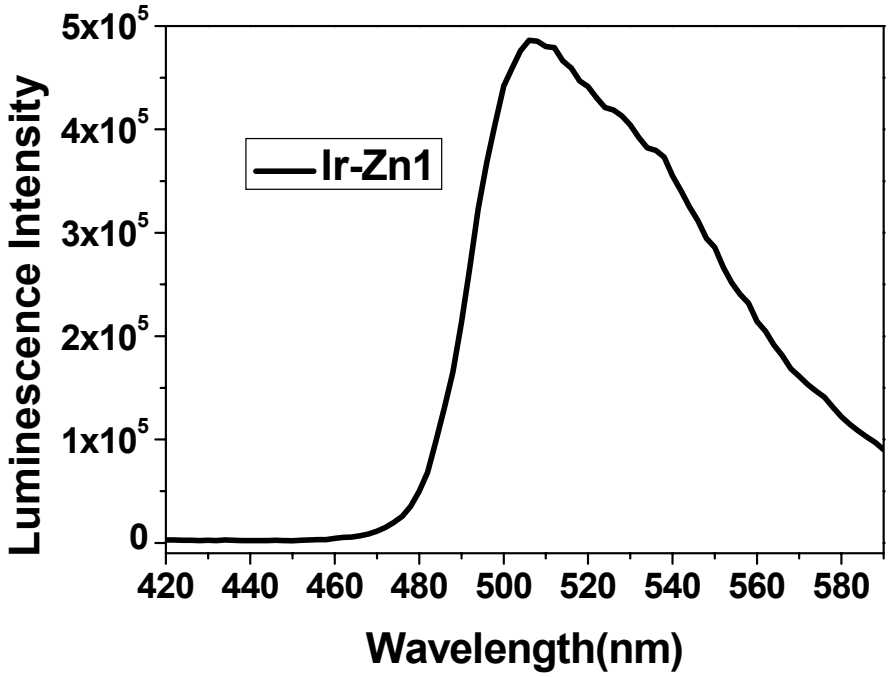

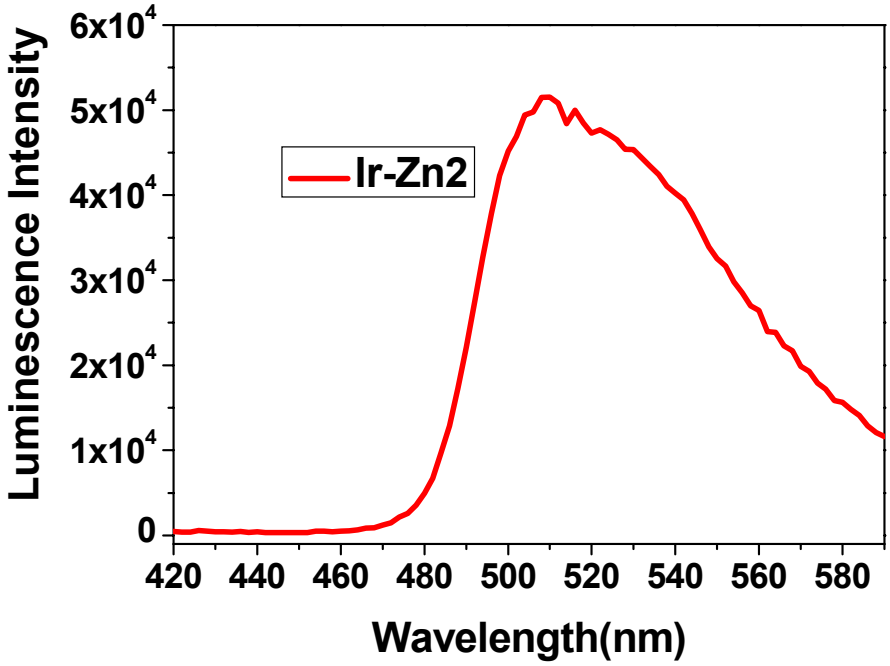

Figure S18 Luminescence spectra of **Ir-Zn1** and **Ir-Zn2**

4.2 Luminescence spectra change upon the bubbling of CO_2 (under a deoxident sieve sorbent) into the Ir-Zn1 solution (1.0×10^{-5} M acetonitrile solution, luminescence spectra were recorded at time intervals of 2 min, excited at 360 nm).

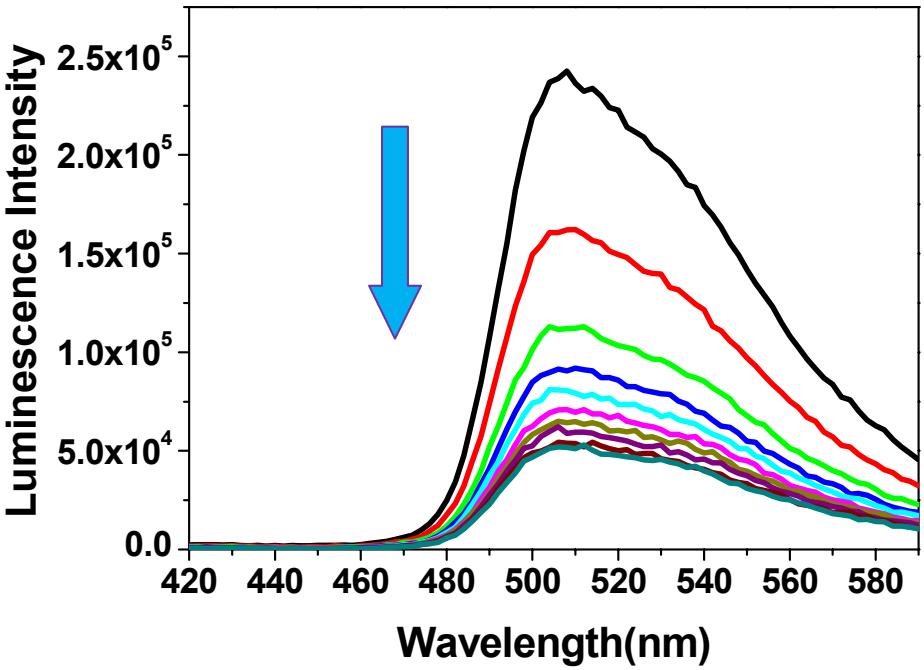

Figure S19 Time-dependent luminescence spectra of **Ir-Zn1** (10 μM) in a CH_3CN solution after the bubbling of CO_2.

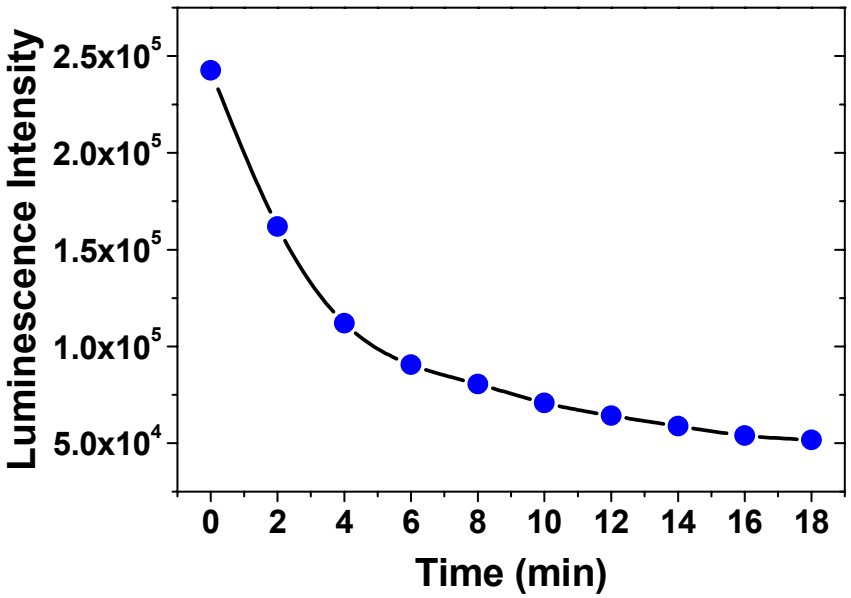

Figure S20 Time-dependent luminescence intensity tracing at 508 nm of **Ir-Zn1** (10 μM) in a CH_3CN solution after the bubbling of CO_2.

4.3 Rate Constant Calculation.

Generally, for the formation of Host-Guest complexation species formed by the cage compound host (H) and the guest (G), the original concentration of the cage being fixed at C_0, and we assume xC_0 to the concentration of complexes species Host-Guest (H-G),

	H	+	G	⇆	H – G
t = 0 min, cage only	C_0				
when G was added, t = t min,	$(1-x)C_0$				xC_0

The measurements are performed under the conditions where the luminescence intensity of the free host (H) in such a concentration is F_0. After addition of a given amount of G, the luminescence intensity (F) of the system is close to (in the dilute solution):

$$F = F_0(1-x) + xF_T \qquad (1)$$

Where F_T is the luminescence of the saturated value in the presence of excess guest.

It is easy to derive the usual equation:

$$(F_0-F) / (F_0-F_T) = x \qquad (2)$$

The first-order dynamics equation:

$$\ln(1-x) = -kt + N \qquad (3)$$

From eqs (2) and (3), we can obtain the equation:

$$\ln[(F-F_T)/(F_0-F_T)] = -kt + N \qquad (4)$$

k can be obtained by a linear analysis of (X) t versus (Y) ln $[(F-F_T)/(F_0-F_T)]$.

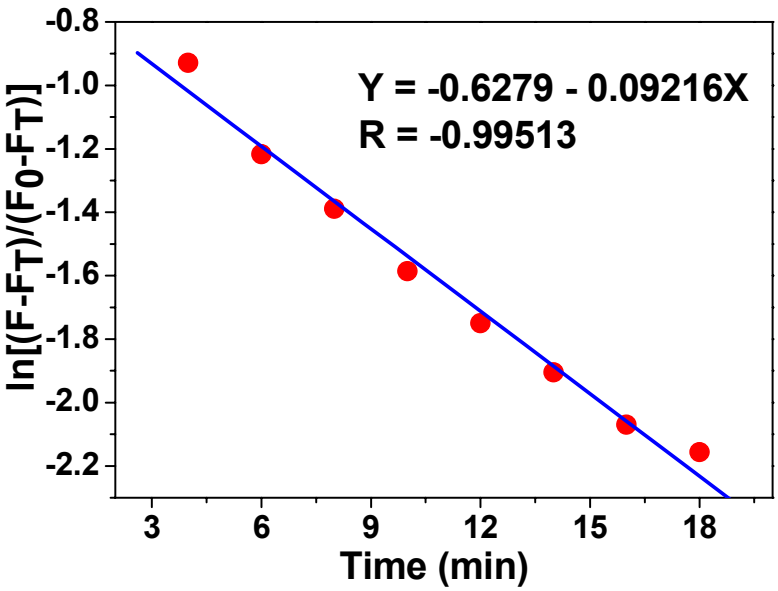

Figure S21 First-order dynamics fitting of luminescence tracing of **Ir-Zn1** upon the bubbling of CO_2. The rate constant calculated $k = 0.092$ min^{-1}.

5. References

[S1] K. A. McGee, K. R. Mann, *Inorg. Chem.* **2007**, *46*, 7800-7809.

[S2] SHELXTL V6.14, Bruker Analytical X-Ray Systems, Madison, WI., 2003.

[S3] G. M. Sheldrick, SHELXTL V5.1, Software Reference Manual, Bruker, AXS, Inc.: Madison, WI, 1997.